



**HAL**  
open science

# Electrode Nanopatterning for Bioelectroanalysis and Bioelectrocatalysis

Umberto Contaldo, Anne De Poulpiquet, Ievgen Mazurenko, Elisabeth Lojou

► **To cite this version:**

Umberto Contaldo, Anne De Poulpiquet, Ievgen Mazurenko, Elisabeth Lojou. Electrode Nanopatterning for Bioelectroanalysis and Bioelectrocatalysis. *Electrochemistry*, 2024, 92 (2), pp.022005. 10.5796/electrochemistry.23-68150 . hal-04464895

**HAL Id: hal-04464895**

**<https://hal.science/hal-04464895>**

Submitted on 19 Feb 2024

**HAL** is a multi-disciplinary open access archive for the deposit and dissemination of scientific research documents, whether they are published or not. The documents may come from teaching and research institutions in France or abroad, or from public or private research centers.

L'archive ouverte pluridisciplinaire **HAL**, est destinée au dépôt et à la diffusion de documents scientifiques de niveau recherche, publiés ou non, émanant des établissements d'enseignement et de recherche français ou étrangers, des laboratoires publics ou privés.



Distributed under a Creative Commons Attribution 4.0 International License

## The 68th special feature "Electrochemistry to Understand Biological Functions"

### Electrode Nanopatterning for Bioelectroanalysis and Bioelectrocatalysis



Umberto CONTALDO, Anne de POULPIQUET, Ievgen MAZURENKO, and Elisabeth LOJOU\*

Aix Marseille Univ, CNRS, BIP, Bioénergétique et Ingénierie des Protéines, UMR 7281,  
31, chemin Joseph Aiguier, CS 70071 13402 Marseille cedex 09, France

\* Corresponding author: [lojou@imm.cnrs.fr](mailto:lojou@imm.cnrs.fr)

#### ABSTRACT

Although intensive research in the bioelectroanalysis domain in the last twenty years led to great improvements in protein-based electrode and device performances, their large application remains limited by their stability overtime under operational and resting conditions. One under-studied issue is the role played by the spatial distribution of enzymes on electrocatalysis. Actually, high fluxes in metabolic pathways involve compartmentalization and spatial organization of active biomolecules. In a mimicking way, it can be expected that controlled localization of proteins on electrode surfaces may play a role in the overall electron transfer processes and bioelectrocatalysis performances. In this short review, we will discuss recent developments in surface patterning allowing to tune in a controlled manner the localization and density of enzymes on the electrode surface. We will investigate how mixed functional layers, electrode and biological materials can serve as protein platforms to provide such electrode patterning.

© The Author(s) 2023. Published by ECSJ. This is an open access article distributed under the terms of the Creative Commons Attribution 4.0 License (CC BY, <http://creativecommons.org/licenses/by/4.0/>), which permits unrestricted reuse of the work in any medium provided the original work is properly cited. [DOI: [10.5796/electrochemistry.23-68150](https://doi.org/10.5796/electrochemistry.23-68150)].



Keywords : Electrode Patterning, Metalloproteins, Bioelectrocatalysis, Spatial Distribution

#### 1. Introduction

Redox enzymes are very active and extremely selective catalysts toward specific reactions allowing their use in bioelectrochemical devices such as biosensors, bioreactors, bioelectrolyzers or biofuel cells.<sup>1-4</sup> Gold and carbon-based electrodes are the most popular materials for their efficient immobilization.<sup>5-9</sup> These materials can be easily chemically modified to introduce functional groups on their surface and tune the interfacial properties for the grafting of enzymes in a conformation suitable for electrocatalysis. Further implementation of porous materials and nanomaterials such as

nanoporous gold, gold nanoparticles (Au NP), or carbon nanotubes (CNT) increases surface area, hence potential anchorage sites for enzyme immobilization, leading to enhanced catalytic currents.<sup>5</sup> Furthermore, depending on their shape and size, nanomaterials can impact the conformation of proteins hence their stability and further their activity.<sup>10</sup> Although intensive research in those areas over the last twenty years has led to great enhancements in catalytic currents and the diversification of potentially catalyzed reactions, the application of enzyme-based bioelectrodes remains limited mainly by their stability overtime under operational and resting conditions. In many cases, immobilized enzymes demonstrate significantly reduced turnover frequencies in comparison to those in solution, which suggests limitations on electrocatalysis from unknown or uncontrolled parameters. Nowadays developed in situ and operando methods coupled to electrochemistry will certainly provide essential data concerning the relationship between electrocatalysis and the loading of enzymes, their conformation or their orientation.<sup>11,12</sup> The



**Umberto Contaldo (Post-Doc, Bioenergetic and Protein Engineering Lab, CNRS, Aix-Marseille University, France)**

Umberto Contaldo was born in 1993. He obtained his master degree in Molecular and Industrial Biotechnology from Alma Mater Studiorum, University of Bologna, Italy in 2018, and PhD degree in Bioinorganic Chemistry from University of Grenoble Alpes, Grenoble, France in 2021. During his PhD project he developed an efficient method for overproducing an engineered carbon monoxide dehydrogenase (CODH). In this way, he achieved the stable and favorable orientation of the CODH on non-covalently functionalized carbon nanotubes (CNTs) with the final integration into an efficient gas-diffusion bioelectrode for the CO/CO<sub>2</sub> interconversion with catalytic efficiency comparable to inorganic catalysts. Since September 2022, he is working on a subfamily of multi-copper oxidase known as copper efflux oxidases (CueOs). CueOs are involved in copper homeostasis, catalyzing the oxidation of Cu<sup>+</sup> to less toxic Cu<sup>2+</sup>.

The aim of the project is to decipher the pathway of copper detoxification through a multimodal approach, from in solution to CNTs immobilization, in order to correlate the *in vitro* knowledge to *in vivo* pathogen resistance to copper. He is member of the French Chemical Society and International Electrochemical Society.



**Anne de Poulpquet (Assistant professor, Bioenergetic and Protein Engineering Lab, CNRS, Aix-Marseille University, France)**

Anne de Poulpquet was born in 1986. She is an assistant professor at Aix-Marseille University, France. She obtained her degree in engineering from the Ecole Centrale de Lyon, Lyon, France in 2010. During her PhD in Aix-Marseille-University, she worked on the development of enzymatic H<sub>2</sub>/O<sub>2</sub> bio-fuel cells. She graduated in 2014. After a post-doc position at the NSysA lab in Bordeaux, France, where she worked on bipolar electrochemistry, electrochemiluminescence and fluorescence microscopy under electrochemical control, she integrated the Bioenergetic and Protein Engineering laboratory, Marseille, in the group lead by Elisabeth LOJOU. Her main research interest is the development of coupled methods for the characterization of enzymatic electrochemical reactivity. She especially focuses on utilizing fluorescence microscopy in operando during the electrochemical experiments.

influence of local environment such as pH or ionic strength, especially relevant when using porous materials, is also expected to be elucidated by coupling electrochemistry to fluorescence confocal microscopy (e-FCM).<sup>13,14</sup>

One under-studied issue, however, is the role of the spatial distribution of enzymes on electrocatalysis. In vivo, high fluxes in metabolic pathways towards optimization of biological synthesis involve different mechanisms including compartmentalization and spatial organization of active biomolecules. One relevant example of enzyme organization is found in respirasomes or cellulosomes, the multi-enzyme nano-factories dedicated to depolymerization of cellulose and hemicellulose.<sup>15</sup> Another example is the metabolic pathway of the Krebs's cycle where enzymes involved in the metabolon are organized in complexes allowing short distances to channel substrates. In this chain, the product of one enzymatic reaction can serve as the substrate for a second enzymatic reaction provided the transport from the first enzyme to the second one is fast enough. Such pathways can be reconstituted on electrode interfaces by fine controlled co-localization of enzymes involved. This so-called cascade of enzymes has been largely investigated as in the case of the coupling of glucose oxidase (GOx) and horseradish peroxidase (HRP) allowing fine product synthesis.<sup>16,17</sup> Hydrogen production by discrete co-immobilization of a [FeFe]-hydrogenase and ferredoxin was also described.<sup>18</sup> Natural metabolic pathways have also been introduced in biofuel cells showing enhanced power output.<sup>19</sup> In such enzymatic constructions, catalytic efficiencies would be enhanced thanks to directed diffusion of intermediary products. However, it was also suggested that scaffolding plays a fundamental role in these multi-enzymatic systems by modifying the local enzyme environment.<sup>20</sup> Otherwise, it was shown an optimum enzyme coverage for enzymatic catalysis at electrodes between rigid monolayer and protein crowding, suggesting a crucial role of protein-protein interactions.<sup>21,22</sup> Indeed, protein-protein interactions may induce protein aggregation following hydrophobic contacts between surface non-polar residues. They may also increase the distance between the active site and the electrode by neighbor obstruction. Also, a change in the polarizability of the environment of proteins with protein coverage, a concept very much like the crowding effect, was proposed to be responsible for a shift in redox potentials.<sup>23</sup>

Tools have been developed to study the electrocatalytic efficiency with high resolution. In particular, methods using scanning electrochemical microscopy (SECM) proved to be able to image enzymatic activity at electrodes at the nanometer scale.<sup>24</sup> Relevant are the works by Matsue and coworkers who used a gold coated capillary to probe the enzymatic activity of GOx and HRP immobilized on a glass slide at the sub-micron scale.<sup>25</sup> This is also the case of the mediator tethered/atomic force microscopy (AFM)-SECM mode developed by Demaille's group that enables the enzymatic activity of surface-attached enzymes to be probed at the nanometer scale.<sup>26</sup> More recently, development of fluorescence confocal microscopy coupled to electrochemistry allowed a

mapping of the enzymatic activity on electrodes.<sup>27</sup> Nevertheless, the strategies to fine-tune the spatial distribution of enzymes on electrochemical interfaces are still at their infancy. To get insight into the localization and density of enzymes on the electrode surface, surface patterning is expected to allow tuning in a controlled manner.<sup>28</sup> It will at the same time provide important information on the role of patterning on enzymatic catalysis. This is the main objective of this review which will discuss recent developments in surface patterning starting from mixed functional layers to DNA origami on electrodes for biomolecule anchorage in a controlled spatial distribution, with a focus on redox enzymes.

## 2. Mixed Functional Layers on Electrodes as Enzyme Platforms

Functional layers for patterning of electrochemical interfaces can be obtained through mixed self-assembled-monolayers, electrografting of diazonium salts or amines, or  $\pi$ - $\pi$  stacking of aromatic compounds. In most reported works in the bio-domain, the main objectives were to avoid steric hindrance or non-specific adsorption in complex media, to allow mimicking a cell membrane or to control and to tune the biomolecule orientation for on/off bioactivity. Mixed functional layers also allowed new insights in local reactivity by permitting control of the functions on the interfaces at the molecular level.

### 2.1 Mixed self-assembled-monolayers

Self-assembled-Monolayers (SAM) constitute a versatile way of surface functionalization including the cases of electrochemical interfaces.<sup>29</sup> One drawback is that some phase aggregation may occur as a function of the ratio of each thiol.<sup>30</sup> The most widely used SAMs consist in an alkyl chain with tunable length carrying on one side a sulfur group for attachment to a gold surface and on the other side a chemical end-function. This function can be hydrophilic or hydrophobic, positive or negative, allowing a specific recognition for the molecule that is targeted. Mixed SAMs appear to be an appropriate strategy for electrode patterning (Fig. 1).<sup>31</sup> They can be obtained by mixing alkane thiols with the same end-functions but with different number of alkyl groups, hence different length of the alkane chain. They can also be formed by mixing alkane chains with different end-functions. Mixed SAMs can also be obtained by



**Ievgen Mazurenko (Researcher, Bioenergetic and Protein Engineering Lab, CNRS, Aix-Marseille University, France)**

Ievgen Mazurenko was born in 1987. He graduated from University of Lorraine (Nancy, France) and Taras Shevchenko National University of Kyiv (Ukraine) in 2013, and earned Doctor of Chemistry (PhD). After several post-doctoral stays in Nancy (France), Marseille (France) and Leeds (UK), he was recruited as Researcher in CNRS (BIP) in 2019. His research interests involve electrochemistry, nanomaterials and immobilized biomolecules with a view to designing various biodevices for energy and substance conversion.



**Elisabeth Lojou (Director of Research, Bioenergetic and Protein Engineering Lab, CNRS, Aix-Marseille University, France)**

Elisabeth Lojou was born in 1961. She obtained her degree in engineering from the National School of Chemistry, Rennes, France in 1985 and PhD degree from Paris XII University in 1988. After a post-doc position in SAFT-Leclanché Company, Poitiers, France, where she developed Li/Liquid cathode batteries, and several positions at CNRS, she integrated the Bioenergetic and Protein Engineering laboratory, Marseille (France) leading a group focusing on the functional immobilization of redox enzymes on nanostructured electrochemical interfaces. Her aim is to understand the molecular basis for the oriented immobilization of enzymes on electrochemical interfaces favoring fast electron transfer process. She developed original electrochemical interfaces for catalytic reduction of metals by cytochromes, as well as for catalytic transformations of H<sub>2</sub> and O<sub>2</sub> by hydrogenases and multi copper oxidases respectively. Recently she designed the first high temperature H<sub>2</sub>/O<sub>2</sub> enzymatic fuel cell. She is currently chair of the International Society of Electrochemistry, division Bioelectrochemistry, treasurer of the bioelectrochemical Society committee, and president of the French Group of Bioelectrochemistry. She is also involved in CNRS committees for permanent researcher recruitment and evaluation. In 2022, she was awarded by the French Chemical Society.

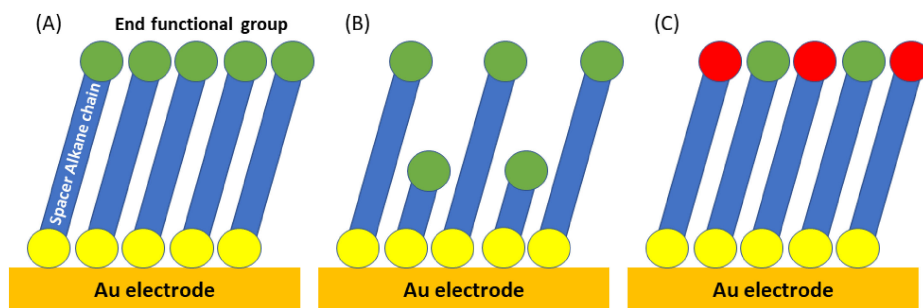


**Figure 1.** Pure SAM electrode components (A); Mixed SAMs with alkane chains of different lengths (B) or with different end functions (C).

lithographic strategies.<sup>24</sup> Depending on the ratio of each thiol, the molecule to be recognized is supposed to be spatially distributed. In all the cases, steric hindrance between immobilized molecules is expected to decrease, inducing an increase in the loading of biomolecules on the surface. A typical case was reported for bovine serum albumin (BSA) covalent attachment with 3,3'-dithiodipropionic acid di(N-hydroxysuccinimide ester) (DSP) self-assembled on gold. By diluting the SAM with 6-mercapto-1-hexanol, BSA binding increased compared to pure DSP layer.<sup>32</sup>

Using mixed SAMs is a strategy that proved to be relevant in many bioelectrochemical studies. Advantageous properties were gained at the scale of the microorganism, cell membrane, DNA or protein. Mayall et al. designed a mixed SAM composed of carboxyl-, ferrocenyl-, and hydroxyl-terminated thiols on gold electrode for detection of Gram-negative bacterial cells thanks to the specific immobilization of Toll-like Receptor-4.<sup>33</sup> The hydroxyl spacer decreased the non-specific adhesion of cells while the ferrocenyl decreased the resistance of the interface. Nucleic acid electroensing on SAMs of thiol-modified DNA was demonstrated to be dependent on the density coverage.<sup>34</sup> Ma et al. further improved the strategy by using a mixed SAM composed of redox and fluorophore labels.<sup>35</sup> Coupling fluorescence microscopy to electrochemistry provided an image of the homogeneity of DNA hybridization on the biosensor as well as information about local environment influence on the detection. Mixed SAMs were especially useful for lipid layer organization on electrodes. Utesch et al. combined Surface Enhanced Infrared Absorption Spectroscopy (SEIRA) measurements with molecular dynamics simulations to investigate the potential distribution across model membranes.<sup>36</sup> Thiol derivatives with different chain lengths were used to design the SAM, creating an aqueous compartment between the islands of the short thiol and the tethered lipid bilayer. Such biomimetic configuration of protein-tethered membrane is promising for elucidating potential dependent processes occurring in/at cell membranes. In this context, a modulation of the distribution of bovine cytochrome *c* oxidase (CcO) orientation in tethered lipid bilayer was demonstrated by first step immobilization on mixed SAMs.<sup>37</sup>

Actually, the CcO was oriented with the cytochrome *c* binding site towards the electrode on hydroxyl (OH) end-group thiol derivative, whereas the opposite was obtained on carboxylate (COO<sup>-</sup>) one. Tuning the ratio of (OH) and (COO<sup>-</sup>) thiols to form the mixed SAM enabled modulation of CcO catalytic activity (Fig. 2).

Other fundamental insights were gained on enzymatic electrocatalysis at the molecular scale thanks to the use of mixed SAMs, ranging from efficient spatial distribution of different enzymes, elucidation of the basis for enzyme immobilization, and reduction of steric hindrance. Mixed SAMs were created based on two thiol derivatives, one carrying a biotin motif and the other an hexa(ethylene glycol) end-function.<sup>38</sup> Once avidin is bound to the

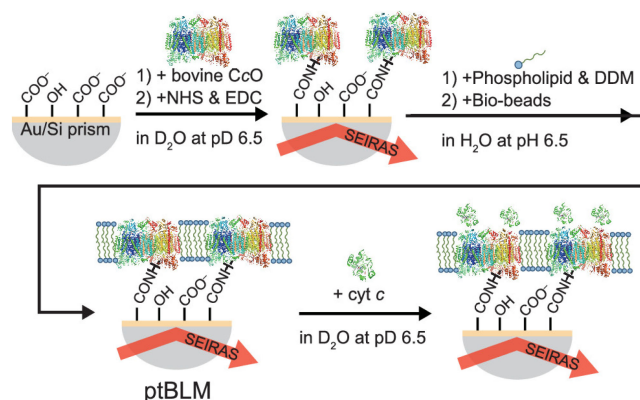


**Figure 2.** Representation of oriented immobilization of bovine CcO on a mixed SAM. Reprinted with permission from.<sup>37</sup> Copyright 2022 American Chemical Society.

former motif, a layer-by-layer construction allowed to spatially immobilize biotin-HRP and biotin-lactate oxidase. The construction was demonstrated to be efficient for lactate detection. Progressive dilution of 11-mercapto-1-undecanoic acid in 11-mercapto-1-undecanol induced SAMs with decreasing negative charge density to be produced.<sup>39</sup> The consecutive decrease of the *Streptomyces coelicolor* small laccase coverage and cyclic voltametry peak currents allowed to prove the electrostatically controlled immobilization of the protein. Sensitive and selective detection of glucose by a biosensor based on cellobiose dehydrogenase (CDH) was realized thanks to enzyme immobilization on gold nanoparticles modified by a mixed SAM.<sup>40</sup> 4-aminothiophenol and 4-mercapto-benzoic acid were used to produce the SAM, offering most probably a platform minimizing protein steric crowding. The idea of bringing enough space for the enzyme to bind was also used by Lokar et al. for glucose sensing by glucose dehydrogenase.<sup>41</sup> In that case, different chain lengths were used.

## 2.2 Mixed organic layers

Another way to obtain patterned and multi-functional surfaces consists in the electrografting of diazonium salts. Although film formation through reduction of diazonium salts is known for more than 30 years, the control of mixed organic films is still challenging. For the readers who are interested in, a comprehensive review was published 5 years ago by J.J. Gooding focusing on aryldiazonium salt based mixed organic layers.<sup>42</sup> Mixed layers can be obtained by electrografting of two different diazonium salts, the surface concentration of one component over the other being mainly controlled by the potential at which each species is reduced. Such a strategy allowed to anchor enzymes such as HRP displaying an efficient interfacial electron transfer while preventing the non-specific adsorption in real samples<sup>43</sup> (Fig. 3).

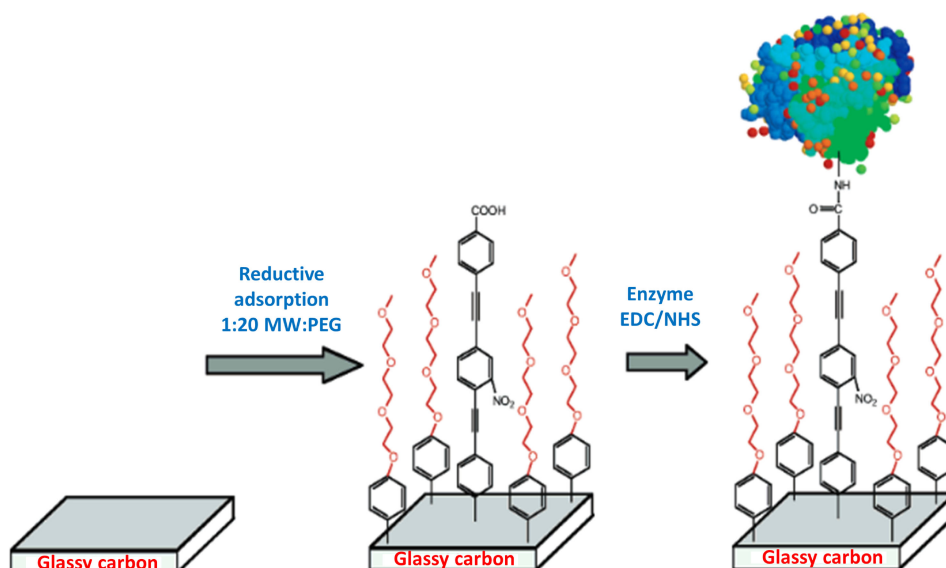


**Figure 3.** HRP attachment to a molecular wire diluted in polyethylene glycol obtained by diazonium salt electrografting. Reprinted with permission from.<sup>43</sup> Copyright 2006 American Chemical Society.

One issue related to film property through diazonium salt reduction is the formation of multilayers which is certainly strongly limiting bio-applications. Strategies have been reported to restrict the film thickness to a monolayer such as the presence of an inhibitor or a bulky protecting group preventing radical induced multilayers. Once the monolayer is formed, a mixed platform can be obtained by grafting two different molecules. A relevant example was described by Cesbron et al. where two acetylene derivatives, including one with a TEMPO motif (2,2,6,6-Tetramethylpiperidinyloxy TEMPO is a stable nitroxyl radical), were clicked to the azide platform made by diazonium salt reduction.<sup>44</sup> The reactivity of the mixed film was then studied for 1-phenylethanol electrocatalytic oxidation as a function of TEMPO density on the surface. The highest reactivity was obtained with a dilution 90/10 TEMPO/acetylene-TEMPO, suggesting the necessity of some flexibility for the TEMPO motif in the reaction with alcohol. Although this particular study does not involve any biological molecules, it may be useful for bioelectrochemical studies in the future. Indeed, TEMPO is a well-known radical used in EPR for spin labelling to characterize protein domain mobility.<sup>45</sup> Since recent works highlight that EPR methodology can be effectively coupled to electrochemistry, this opens avenues towards redox-dependent protein domain dynamic studies.<sup>46</sup>

Electro-oxidation of amines of various chemical composition constitutes another way for designing patterned electrodes. A mixed organic layer was obtained by Al-Lolage et al. by oxidation of an amine-based linker on CNTs for enzyme attachment diluted by another type of amine as passivating layer. This strategy allowed the specific coupling of CDH and bilirubin oxidase (BOD) in a given orientation for electrocatalysis through covalent coupling of maleimide groups on the electrode surface and an engineered cysteine residue at the enzyme surface.<sup>47,48</sup>

### 2.3 Mixed $\pi$ - $\pi$ stacking on aromatic substrates

$\pi$ - $\pi$  stacking on aromatic platforms can alternatively be used to design mixed layers adaptable to protein immobilization. Such a procedure has been widely carried out for enzyme immobilization on CNT-based electrodes.<sup>49</sup> Patterning of the surface is expected to avoid steric hindrance of the protein. As an illustration, the histidine-tagged (His-tag) multicopper oxidase from *Pyrobaculum aerophilum* (McoP) was immobilized on a CNT-film via the affinity interaction between the His-tag and a nitrilotriacetic pyrene

derivative with coordinated  $\text{Ni}^{2+}$  (PBSE/NTA/ $\text{Ni}^{2+}$ ).<sup>50</sup> A catalytic current resulting from a direct wiring of the enzyme to the surface was observed. This result was explained based on the swinging ability of the enzyme on the surface. The enzyme surface coverage was varied by introducing a spacer preventing enzyme anchorage (Fig. 4). Current densities were enhanced as a result of a decrease in enzyme density and increase in enzyme swinging ability as elucidated by QCM.

## 3. Electrode Material Patterning

In the section above, patterning was realized by chemical modifications of a surface with given structural and chemical properties. An alternative is to tune the electrode material itself for patterning.

### 3.1 Electrode patterning by lithography procedures

Maskless and template-assisted lithographic methods offer many possibilities for surface patterning. They are widely applied to advanced electronic devices. Depending on the method used, i.e. ion beam, electron beam, interference or nanoimprint lithography, different surfaces can be patterned with sub-10 nm resolution. More than 20 years ago, Wittstock's group highlighted the possibility of spatially distributing enzymes on an electrode through lithography procedures.<sup>24</sup> Ten years later, electrode nanostructuring was achieved by nanoimprint lithography (NIL) of polymer sheets, and tested for oxygen reduction reaction (ORR) by *Myrothecium verrucaria* BOD (*Mv* BOD).<sup>51</sup> The induced nanocavity centers were separated by a distance about 300 nm (Fig. 5). The embedding of the enzymes in the nanocavities was proposed to be responsible for stability enhancement of the bioelectrode. However, nano-patterning did not lead to a drastic improvement of the catalysis kinetics. More recently, ordered nanoelectrode arrays were designed by thermal nanoimprinting lithography on glassy carbon, yielding nanoelectrodes with a radius of 145 nm arranged in a square lattice with 770 nm pitch.<sup>52</sup> Such nanoelectrode arrays were evaluated for redox mediator electrochemistry in view of enzymatic reactions.

### 3.2 Electrode patterning by tailoring the porosity of the electrode

Porous electrodes from various chemical composition and hierarchical porosity have been designed for many years as suitable

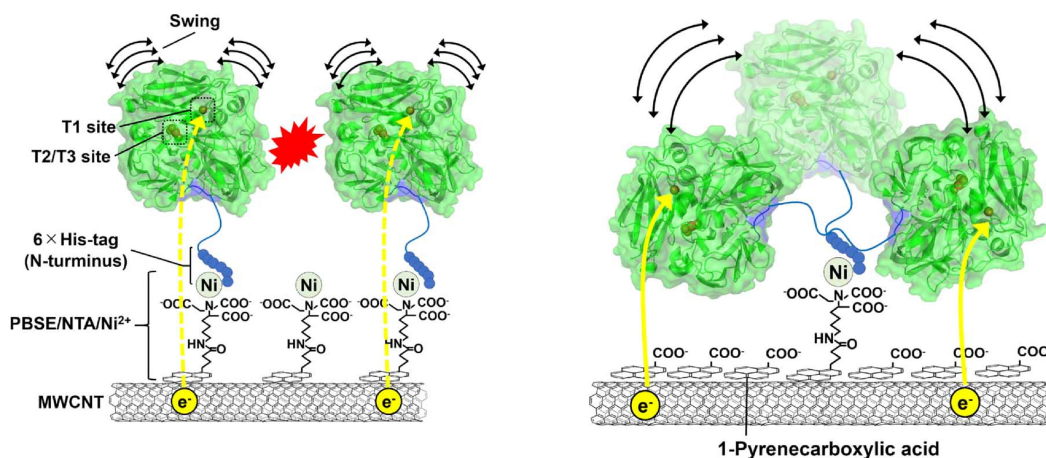


**Figure 4.** Effect of enzyme coverage of *Pyrobaculum aerophilum* multi copper oxidase (McoP) on enzyme swing ability which controls electrocatalysis. Reprinted with permission from.<sup>50</sup> Copyright 2021 IOP Publishing Ltd, England.

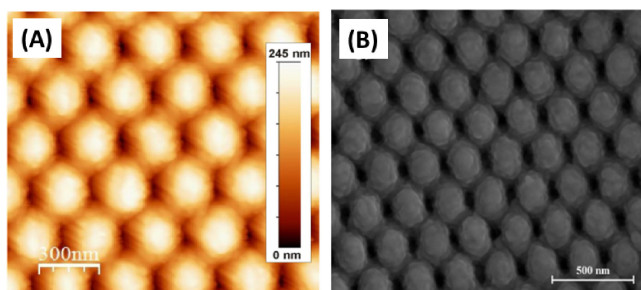


**Figure 5.** AFM (A) and SEM (B) images of NIL/Au electrode. Adapted from 51, Copyright 2015.

platforms allowing enzymes embedding and substrate diffusion.<sup>53,54</sup> However, only a few works focused on the spatial distribution of enzymes in such porous electrodes. Wu et al. incorporated GOx attached to polystyrene nanospheres (PS) in hollow fiber membrane (HFM) on which poly-(3,4-ethylenedioxythiophene) (PEDOT) was synthesized.<sup>55</sup> HFM displays a unique high surface area with pores decreasing from  $\mu\text{m}$  size in the inner surface to less than 100 nm size in the outer surface. The authors showed that the enzyme spatial distribution throughout the HFM skeleton can be modulated by tuning flow velocity of the filtration process. In particular, the highest stability and activity was observed when the enzyme was uniformly distributed in the HFM pores.

Mazurenko et al. proved that hydrogenase molecules for  $\text{H}_2$  oxidation were homogeneously distributed in a millimeter size carbon felt functionalized by CNTs.<sup>56</sup> This conclusion was obtained based on the catalytic current obtained in full and half size felt. Following a similar strategy, Mano et al. imaged the embedding of *M. oryzae* BOD in fibers obtained by a wet spinning process and further modified by CNTs.<sup>57</sup> Labelled-BOD images obtained by confocal fluorescence microscopy proved the localization of the enzyme in the whole volume of the fibers, although the results could not assess whether these enzymes are catalytically active or not. Moreover, none of these studies could reach a resolution at the molecular scale.

Mesoporous silica is another relevant material for enzyme embedding in a controlled manner. Dendritic mesoporous silica nanoparticles (DMSNs) were used for incorporation of GOx and chloroperoxidase (CPO) in the material channels.<sup>58</sup> The authors focused on the role played by the channel size and enzyme

distribution on the enzymatic cascade reaction. DMSNs displayed channels in the range 11–17 nm. The efficiency of the cascade reaction was improved by decreasing the channel size, hence the distance between the enzymes. Three enzymes operating in cascades for methanol production from  $\text{CO}_2$  were co-immobilized in siliceous mesostructured cellular foams (MCF).<sup>59</sup> Labelling of the enzymes with a fluorescent dye allowed to localize them into the particle, and to study their inter-distance with Förster resonance energy transfer (FRET). A higher catalytic efficiency was obtained when the enzymes were sequentially incorporated in the material according to their size compared to the order they operate in the cascade, suggesting a role of steric hindrance.

### 3.3 Electrode patterning through nanoparticle distribution

Nanoparticles (NPs) have been widely used as platforms for protein anchorage. In addition to the ability to form nanostructured electrodes, NPs themselves were proved to enhance the enzymatic activity depending on NP size and enzyme crowding on the surface.<sup>60</sup> Tuning the ratio of enzyme/NP also allowed to prove that the efficiency of enzyme cascades organized on NPs are dependent on the distance between each enzyme.<sup>61</sup> For bioelectrocatalysis, in most cases, AuNPs are drop-casted on an electrode forming multiple layers. Electrocatalytic currents are accordingly increased as a consequence of the increase in the surface area.<sup>62,63</sup> Even in this simple case, interesting information can be obtained by modifying the size of AuNPs forming the layers. As an illustration, Suzuki et al. synthesized AuNPs of three different sizes, namely 7, 15 and 70 nm.<sup>64</sup> AuNP solutions were drop casted forming multiple layers on polycrystalline Au. While no organization of the NP network was achieved, it was proposed that the catalytic current for ORR by *Mv* BOD or fructose oxidation by D-fructose dehydrogenase was only dependent on the space between each NP enabling enzyme diffusion throughout the NP-based film.<sup>64</sup>

Nonetheless, depending on the way they are synthesized, NPs can be spatially disposed in a controlled way on the electrode surface. Lee et al. synthesized AuNPs by deposition of Au films with tunable thicknesses on Si, followed by sintering at temperatures above  $500^\circ\text{C}$ . AuNPs with sizes from 10 to 80 nm spatially distributed on Si were obtained.<sup>65</sup> PQQ-dependent glucose dehydrogenase was engineered with a gold binding peptide in order to anchor the enzyme on the induced gold nano-islands excluding non-specific adsorption on bare silicon. Such a platform allowed controlling inter-enzyme spacing (Fig. 6). The location of the gold binding peptide was chosen to favor close connection of the FAD site with the electrode. Hence, a direct catalytic process was

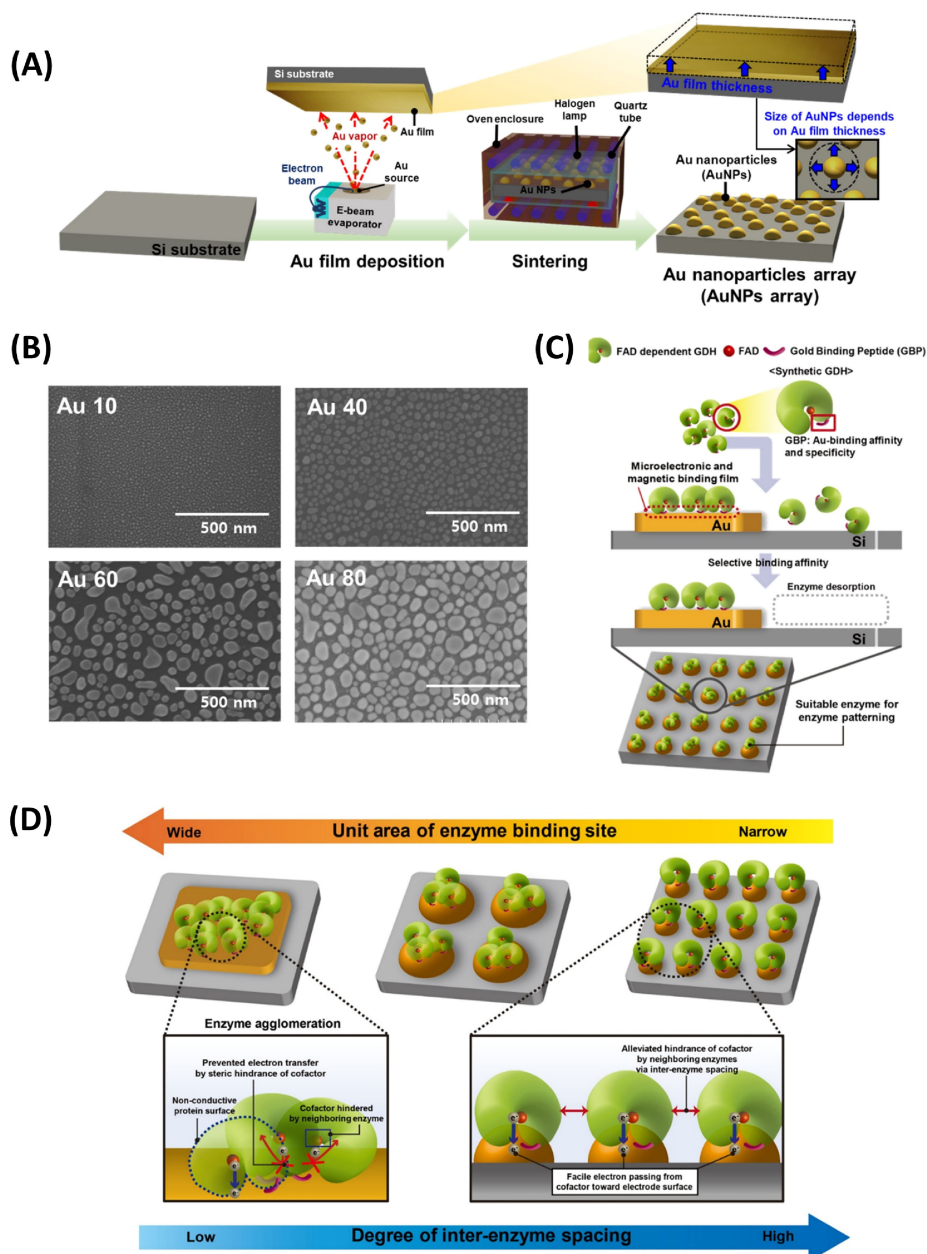


**Figure 6.** Spatially distributed AuNPs on Si as a platform for Au-peptide engineered GDH. (A) fabrication process of AuNPs; (B) SEM images of AuNPs; (C) binding of Au peptide GDH; (D) scheme of steric hindrance tuning and consecutive electron transfer for bioelectrocatalysis. Adapted with permission from.<sup>65</sup> Copyright 2019 Elsevier.

obtained, although not well defined, with currents three times higher than in the absence of the peptide. It was shown that the onset potential for glucose oxidation shifts in the positive direction with the AuNP size. Kinetic analysis further showed higher affinity and catalytic current magnitude on AuNPs patterned electrode compared to a planar electrode. The electrochemical results were analyzed in terms of interspacing distance between neighboring enzymes. One consequence is the decrease in protein agglomeration, hence the enhancement of the number of electroactive enzymes. However, AuNP curvature was not considered in the current work although it may play a crucial role.

We used laser ablation of Au films to synthesize AuNPs with controlled sizes and distribution on ITO electrodes<sup>66</sup> (Fig. 7). AuNPs as hemispheres were mainly observed, and we showed that the density of AuNPs increased with decreasing Au film thickness, while the AuNP diameter increased with the initial Au film thickness. AuNPs with diameters increasing from 100 to 230 nm

were obtained by increasing the Au film thickness from 20 to 40 nm. A broader range of nanoparticle size distribution was also observed for thicker films compared to thinner ones. Thiol modification of AuNPs allowed enzymes to be immobilized in a specific orientation for O<sub>2</sub> direct reduction. Two different multi-copper oxidases were used, namely *Mv* BOD and *Thermus thermophilus* Laccase (*Tl* Lac). The efficient and stable bioelectrocatalytic O<sub>2</sub> reduction on AuNPs with a specific orientation of MCOs as a function of thiol chemistry is in agreement with previous data on planar gold. However, the size of AuNPs (>150 nm) prevented any fundamental studies on the enzyme spatial distribution. Furthermore, as the density of AuNPs varied with the diameter, it was not possible to correlate any of these parameters with the electrocatalysis efficiency. One more issue was linked to the electroactivity of the enzymes on ITO which complicated the analysis of the entire signal.

To overcome these issues, we turned to another material for AuNP synthesis. Titanium nanodimples obtained from chemical

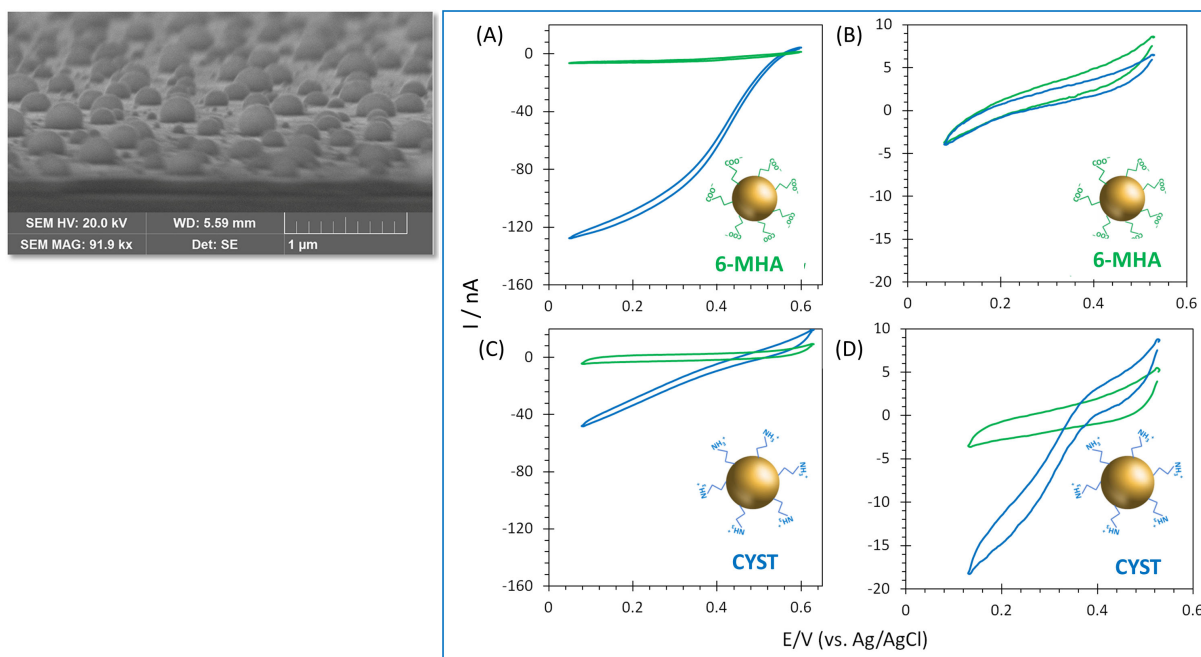


**Figure 7.** AuNPs spatially distributed on ITO for enzymatic  $O_2$  reduction. (Left): SEM images of AuNPs; (right) CVs obtained under  $N_2$  (green) and  $O_2$  (blue) on (A,B) 6-MHA and (C,D) CYST functionalized AuNP@ITO (from Au film thickness of 30 nm) electrodes with adsorption of *Mv* BOD (A,C) or *Tt* Lac (B,D). Reprinted with permission from.<sup>66</sup> Copyright 2020 Frontiers media SA.

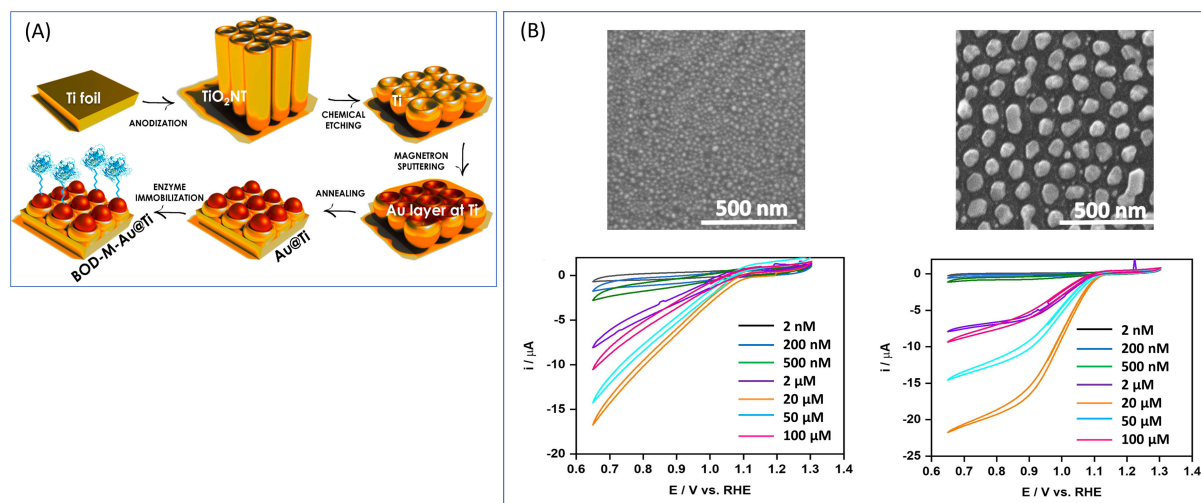


**Figure 8.** Spatially distributed AuNPs in  $TiO_2$  nanodimples. (A) scheme of AuNP synthesis; (B) Size and distribution (top) and catalytic  $O_2$  reduction (bottom) on AuNPs obtained from 2 nm (left) and 10 nm (right) Au films. Adapted with permission from.<sup>68</sup> Copyright 2024 Elsevier.

etching of  $TiO_2$  nanotubes were covered by thin films of Au.<sup>67,68</sup> After annealing process, AuNPs were formed with controlled spatial distribution and diameter sizes between 40 and 90 nm depending on the initial Au film thickness. *Mv* BOD immobilization on so-obtained platforms revealed that ORR occurred only on the AuNPs, with exclusion of the inter-AuNPs material composed of  $TiO_2$  (Fig. 8). Interestingly, the catalytic current was demonstrated to be highly stable even at high ionic strengths. We then focused on the smallest AuNP size, suitable to host a single enzyme molecule. In this particular case, the catalytic wave shape and its modeling indicated a slow electron transfer process, which was explained by the presence of an isolating  $TiO_2$  layer in the surrounding of the AuNPs.

#### 4. Biological Material for Enzyme Spatial Distribution: Microbial Surface Displays, Virus Scaffold and DNA Origami

##### 4.1 Microbial surface displays

A variety of proteins attached to surfaces of microbial cells were proved to be able to serve as anchors for the display of foreign proteins.<sup>69</sup> This is the basis of molecular display technology. Since its initial development in the 1980s, the kind of microbial cells suitable as host strains for protein display has been diversified. Proteins of interest are produced by genetic engineering as a fusion protein of the cell wall proteins. Interestingly, expression and production of these proteins occur simultaneously to their attachment on the cell wall components through the anchoring motif fused

to their N- or C- terminus. Enzymes displayed on microbial surfaces often demonstrate higher stability and activity than enzymes in solution.<sup>70,71</sup> Applications in electrosynthesis with increasing yields were reported by surface display of enzymes on the gram negative cells of *Escherichia coli*.<sup>72</sup> In addition, recycling of the cofactor NADPH was successfully achieved thanks to bacterial surface display immobilization of redox enzymes.<sup>73,74</sup> This technology is particularly useful to reconstitute macromolecular complexes on a surface for metabolic processes. A seminal illustration is the display of a cellulosome-like complex of enzymes on the surface of the gram positive cell *Lactococcus lactis*, a first step toward degradation of cellulose into fermentable sugars.<sup>75</sup> A three-enzyme cascade was also site-specifically assembled through affinity reactions on the surface of a yeast cell. CO<sub>2</sub> production from methanol was 5 times enhanced with enzymes co-localized in comparison with the use of the 3 enzymes non-specifically immobilized.<sup>76</sup>

Thus, microbial surface display appears as an elegant strategy to spatially distribute proteins on a surface such as an electrode. One further advantage of the technique consists in site-specifically wiring of the surface-display proteins to electrodes. In the bioelectrochemistry domain, the most widely used microbes for surface display have been *E. coli* and the yeast *Saccharomyces cerevisiae*, with ice nucleation protein (INP) and  $\alpha$ -Agglutinin or a-agglutinin as typical cell-wall anchoring domains, respectively<sup>77</sup> (Fig. 9).

The surface display technology has been used for electrochemical biosensing, showing in many cases increased specificity and reactivity.<sup>78–80</sup> It has also been employed for energy production through biofuel cells.<sup>81–84</sup> More recently, the technology took profit of enzyme cascades for full oxidation of fuels and to spatially control the localization of enzymes involved in the cascade reactions. One objective was to optimize the substrate diffusion. Szczupak et al. designed a biofuel cell in which the cathode and the anode are based on enzymes displayed on the electrosome through specific interactions between the cellulosomal scaffolding protein and enzyme cascades.<sup>85</sup> The anode consisted of surface-display cascade enzymes for ethanol oxidation, while the cathode relied on displayed copper efflux oxidase (CueO), an O<sub>2</sub> reducing enzyme, limiting competitive O<sub>2</sub> consumption by yeasts. In this preliminary work, however, spatial control of the enzymes involved in the

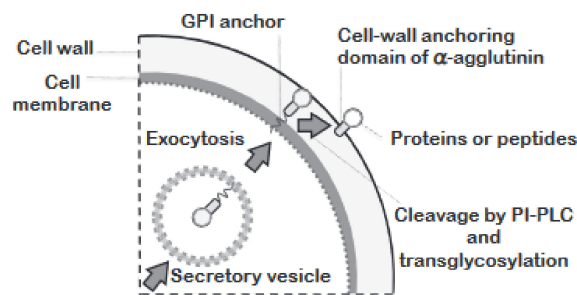


**Figure 9.** Principle of yeast surface display technology. Adapted with permission from.<sup>77</sup> Copyright 2014 SOC ANTIBACTERIAL & ANTIFUNGAL AGENTS, Japan.

cascade was not considered. This spatial localization control was achieved in a work reporting the use of two sequential enzymes, glucoamylase (GA) and GOx, immobilized on a yeast cell surface through an  $\alpha$ -agglutinin receptor as the anchoring motif with cohesin–dockerin interaction<sup>86</sup> (Fig. 10). The co-displayed enzymes were thereafter immobilized on glassy carbon electrodes. It was shown that the catalytic activity was highly dependent on the assembly protocol, especially on the enzyme molecular size, enzyme order and stoichiometry. More precisely, when the GA fusion protein was displayed before GOx, the reaction rate was 26 % higher than when the reverse order was used. The reaction rate was also lower when both enzymes were simultaneously displayed on the scaffold. The different sizes of the enzymes may account for this reactivity, GOx preventing the assembly of GA on the scaffold by steric hindrance. The overall reaction rate was much higher than obtained with free enzymes, suggesting that the controlled localization of enzymes enhances the metabolic flux. Otherwise, the ratio of GA to GOx on cell surface was demonstrated to be crucial and determined by GA starch hydrolysis limiting step. Such a rational assembly was used for starch/O<sub>2</sub> biofuel cell design, highlighting the highest performance with a ratio and order of co-displayed enzymes in the order yeast/GA/GOx/GA.

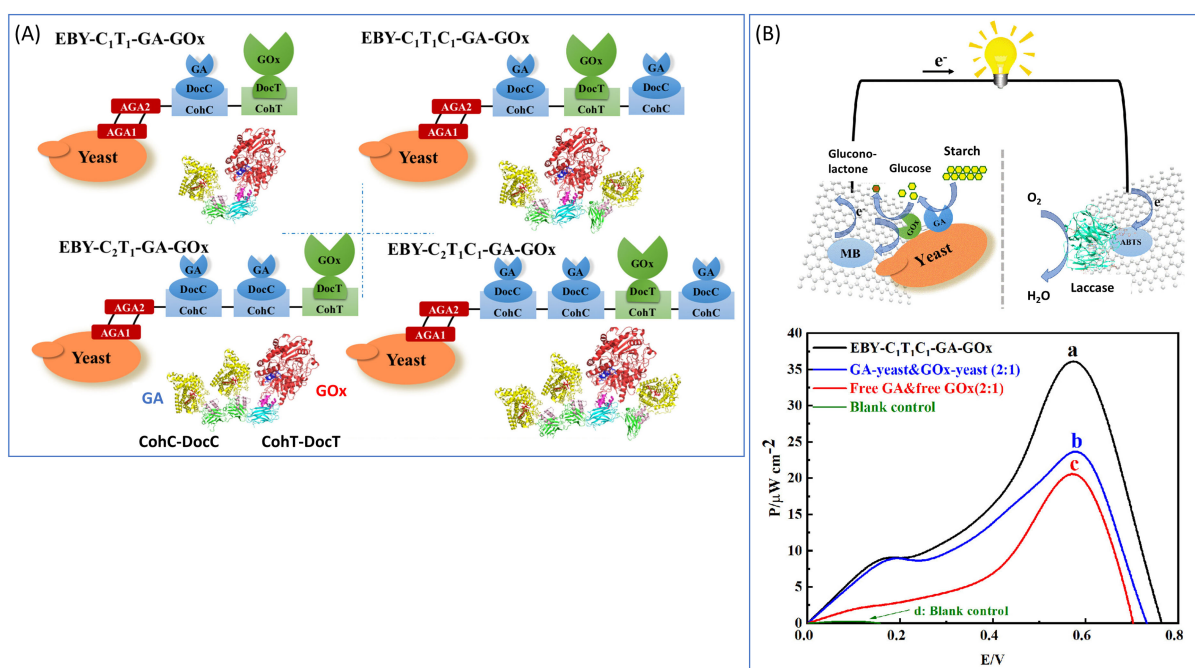


**Figure 10.** (A) Yeast surface co-display of GA and GOx on bifunctional scaffold. (B) Scheme of the starch/O<sub>2</sub> biofuel cell (top) and fuel cell performances (bottom) as a function of the assembly method. Adapted with permission from.<sup>86</sup> Copyright 2020 American Chemical Society.

## 4.2 Virus scaffold

Viruses are self-replicating infectious nanoobjects presenting defined different shapes (filamentous, spherical, icosahedral, rod) and an ordered architecture<sup>87</sup> (Fig. 11). Harmless viruses from plants or bacteriophages can be used as building blocks for self-assembly of metallic nanoparticles in a configuration where plasmon coupling occurs, then allowing subsequent biosensing.<sup>88</sup> They also act as an attractive platform for spatially controlled enzyme immobilization. One additional interest in using virus scaffolds is the possibility of their oriented assembly on an electrode. As an example, the tobacco mosaic virus (TMV) is a 300 nm tube whose outer surface presents thousands of sites precisely and regularly distributed that can act as binding sites for biomolecules. Hence, an electrochemical sensor was developed based on TMV as a nanocarrier allowing the binding of a high amount of precisely positioned GOx.<sup>89</sup> TMVs were also aligned on a gold electrode

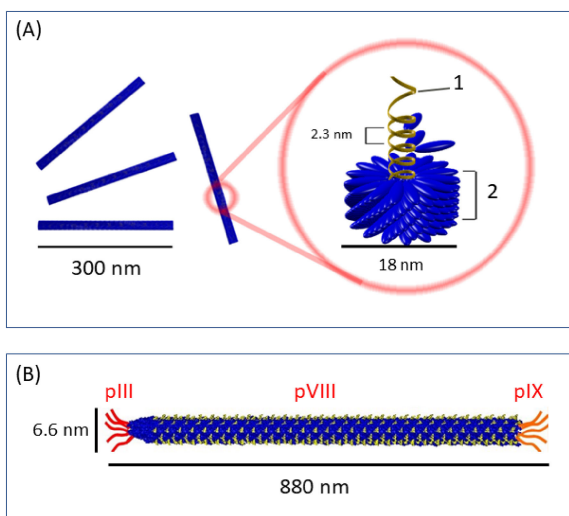


**Figure 11.** Schematic structures of TMV (A) and M13 (B) virus particles allowing platforms for spatial controlled immobilization of biomolecules. In (A), 1 is for nucleic acid and 2 for protein coat (capsid); in (B) pIII, pVIII and pIX are the major coat proteins. Adapted with permission from.<sup>92</sup> Copyright 2012 IOP Publishing Ltd.

allowing spatial distribution and proximity of enzyme cascades, inducing efficient conversion of S-adenosylmethionine to auto-inducer-2 (AI-2).<sup>90</sup> Another example is M13 virus, a filamentous bacteriophage, on which gold NPs were assembled serving as anchorage for high loading of GOx.<sup>91</sup>

*fd* bacteriophage is very close to M13, and is composed of 2700 coat proteins (CPs) forming a 900 nm capsid, with distinct proteins at each extremity. It has been exploited for fundamental studies of bioelectrocatalysis at the nanoscale in the Demaille's group.<sup>93</sup> This group developed elegant tools based on AFM coupled to electrochemistry to highlight some fundamental knowledge on enzymatic electrocatalysis that can be gained when such virus architectures are immobilized on electrodes. In particular, thanks to sub-particle resolution, they showed that it is possible to determine the spatial distribution of enzymatic electroactivity over individual virus particles.<sup>94</sup> The authors studied enzymatic glucose oxidation by GOx or quinoprotein glucose dehydrogenase (PQQ-GDH) immuno-immobilized on *fd* bacteriophage particles assembled on a gold electrode<sup>95,96</sup> (Fig. 12). Interestingly, when PQQ-GDH was co-immobilized on the virus scaffold with a suitable redox mediator for glucose oxidation, enhanced turnover rates were obtained compared to enzymes immuno-immobilized on the gold electrode. Combining AFM and SECM, the faster electron transfer rate could be related to the confinement at the nanoscale of the redox mediator/enzyme couple. Further, the higher enzymatic activity observed in the middle of the *fd* scaffold could be related to electron hopping between the redox moieties along the viral particles.<sup>97</sup> It was also demonstrated that while oriented virus allows full immunodecoration, hence higher enzyme coverage compared to randomly dispersed virus, the kinetics of the bioelectrocatalytic reaction is enhanced on the randomly oriented viruses compared to oriented one. Finally, to elucidate the role of the properties, length and shape of viral particles on the spatial distribution of electrocatalysis, the same procedure was used to immobilize PQQ-GDH on shorter TMV virus.<sup>98</sup> Kinetic analysis of the enzymatic reaction was also performed by regioselective immuno-decoration of the icosahedral grapevine fanleaf viral particle using a novel class of antibodies, namely the nanobodies.<sup>99</sup> A dependence of viral type on substrate inhibition was revealed. All of these studies clearly highlight the differences in enzymatic activities when analyzing at the single particle level compared to the bulk ensemble.

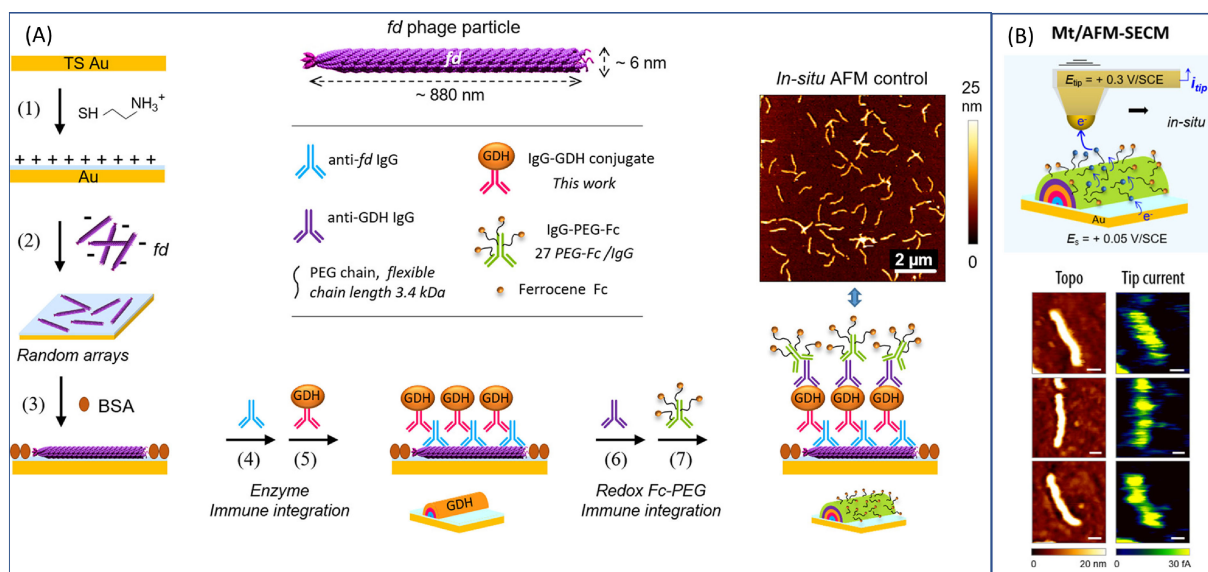


**Figure 12.** (A) Principle of the assembly of enzymes on virus scaffold; (B) Combined AFM and SECM allows to visualize the topography and catalytic current generated by co-immobilization of PQQ-GDH and redox mediator on the virus scaffold. Adapted with permission from.<sup>96</sup> Copyright 2019 American Chemical Society.

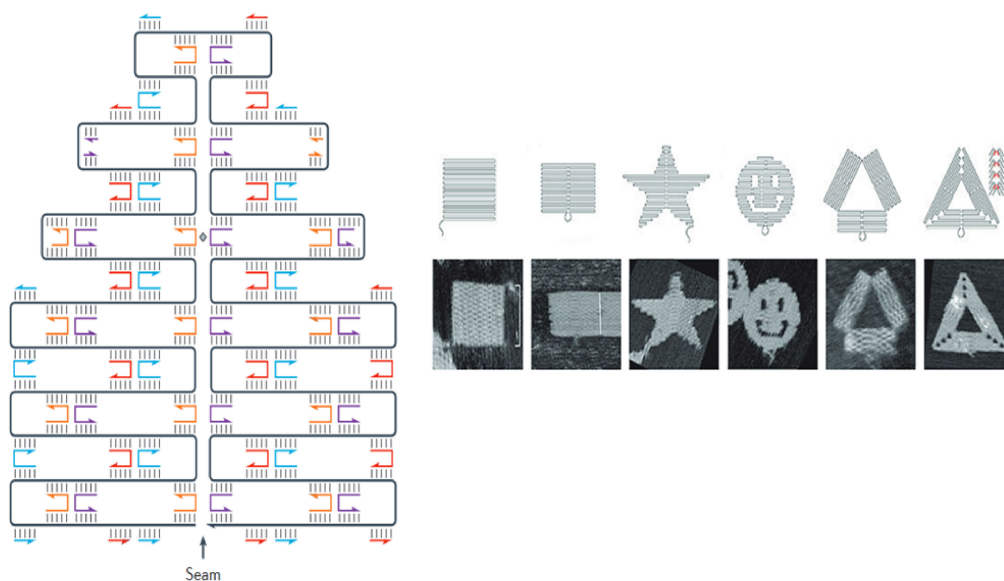


**Figure 13.** DNA origami scaffolding based on a long DNA strand folded thanks to small staple strands to give the desired shapes imaged by AFM. Scale bars are 100 nm. Adapted with permission from.<sup>102</sup> Copyright 2018 Nature.

#### 4.3 DNA origami

DNA origami methodology is an elegant bottom-up approach to elaborate spatially well-controlled 2D or 3D nanostructures.<sup>100</sup> The self-assembly of DNA provides a highly tunable platform through its programmable genetic code. It was first developed by Rothemund in 2006,<sup>101</sup> who proposed a versatile ‘one-pot’ method for folding a long, single strand of DNA into a desired pattern thanks to the addition of short strands acting as staples. Each of hundreds of short strands are complementary to one site of the long strand, leading to localized hybridization. Patterns such as squares, triangles and five-pointed stars with a spatial resolution of about 6 nm can thus be obtained resembling Japanese origamis<sup>102</sup> (Fig. 13). Although this technology may suffer from lower stability than viral proteins scaffold, no doubt it offers an attractive playground towards a diversity of platforms suitable to tune and control biomolecule spatial immobilization.<sup>88,103</sup>

DNA origamis were reported to serve as support for NPs, allowing to control the spatial repartition of attached enzymes.<sup>104</sup> DNA origamis were widely demonstrated to be suitable for controlled immobilization of cascade enzymes.<sup>105,106</sup> A tubular nanoreactor was fabricated based on two 3D DNA origami building blocks anchoring GOx and HRP then glued together via DNA base pairing.<sup>107</sup> The formation of tetramethylbenzidine diimine was accelerated thanks to the nanoconfinement of the two enzymes. The photoregulation of enzyme cascade activity by anchoring of photoresponsive azobenzene molecule and by precise control of inter-enzyme distance on DNA origami was otherwise described.<sup>108</sup> The immobilization of GOx and HRP enzymes through conjugation to DNA origami tiles allowed the study of the effect of the inter-protein distance on the activity.<sup>109</sup> The activity increased compared to non-scaffolded enzymes and was shown to be inter-enzyme distance dependent. For distances about 10 nm, the connection of the hydration shell of the two enzymes restricting the diffusion of H<sub>2</sub>O<sub>2</sub> from one enzyme to the other was proposed to be at the origin of the increase of activity. For distances greater than 20 nm, the enhancement of activity decreased however, suggesting limitation by another diffusion mechanism. Actually, the mechanisms under the increased activity observed with scaffolded enzymes in a cascade is still a matter of debate.<sup>106,110</sup> Local environment, and affinity of the intermediates with the scaffold platform would be involved in addition to the inter-enzyme distance.

This technology should be very attractive in view of bioelectrocatalysis providing suitable anchorage of DNA origamis on electrochemical interfaces. Nevertheless, only few works report DNA origami construction on electrodes for further assembling of redox proteins. Note however that apart from origami, DNA can serve as an efficient platform to assemble enzymes through fusion to sequence-specific DNA-binding protein. A seminal work was reported by Xia et al where alcohol dehydrogenase and aldehyde dehydrogenase were attached to DNA scaffold in a controllable manner.<sup>111</sup> By incubation with a CNT dispersion, this strategy allowed the design of a cascade enzyme electrode presenting fine substrate channeling. Ge et al. controlled the position of cytochrome *c* inside or outside a DNA tetrahedron deposited on a Au electrode.<sup>112</sup> A higher electron transfer rate and positive shift of the redox potential was attributed to the charged environment provided by the DNA cage. Furthermore, the tetrahedron allowed tuning the position of cytochrome *c* relative to the electrode. Regarding DNA origamis, nanoimpact electrochemistry was developed to investigate their properties thanks to the intercalation of methylene blue,<sup>113</sup> opening the way to electrochemical nanosensors. miRNA-21 detection was achieved thanks to indirect measurement by intercalated methylene blue (MB) redox probe of the hybridization with ssDNA decorating a cross-shaped DNA origami<sup>114</sup> (Fig. 14). Taking advantage of the controlled density of ssDNA on the DNA origami, such an architecture is supposed to enable detection of large biomolecules.

Triangular DNA origamis attached to a Au electrode were used to precisely localize multiple target-binding sites spaced over the length scale required for electrochemical detection of various analytes.<sup>115</sup> A DNA-origami based enzymatic cascade electrode was reported by Ge et al, based on a rectangle DNA origami with spatially localized GOx and HRP attached to a Au electrode.<sup>116</sup> The DNA anchorage to the SAM-modified Au electrode was achieved by placing DNA strands with thiol groups on the backside of the DNA origami (Fig. 15). The coverage of origami tiles on Au was found to be close to 50%. Four different distances separating the enzyme on the DNA origami were then probed. In the case of the smallest distance, it was found that steric hindrance decreases the co-assembly of GOx and HRP. Nevertheless, this shortest distance induced the highest electrochemical activity, also 20 times higher than that obtained with free enzymes. Another interesting feature of

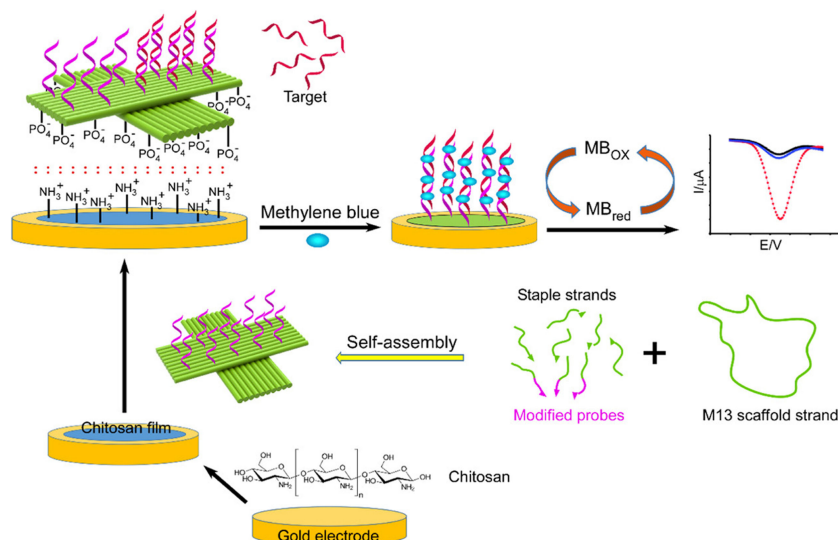


**Figure 14.** Electrochemical detection of miRNA by DNA origami. Reprinted with permission from.<sup>114</sup> Copyright 2019 American Chemical Society.

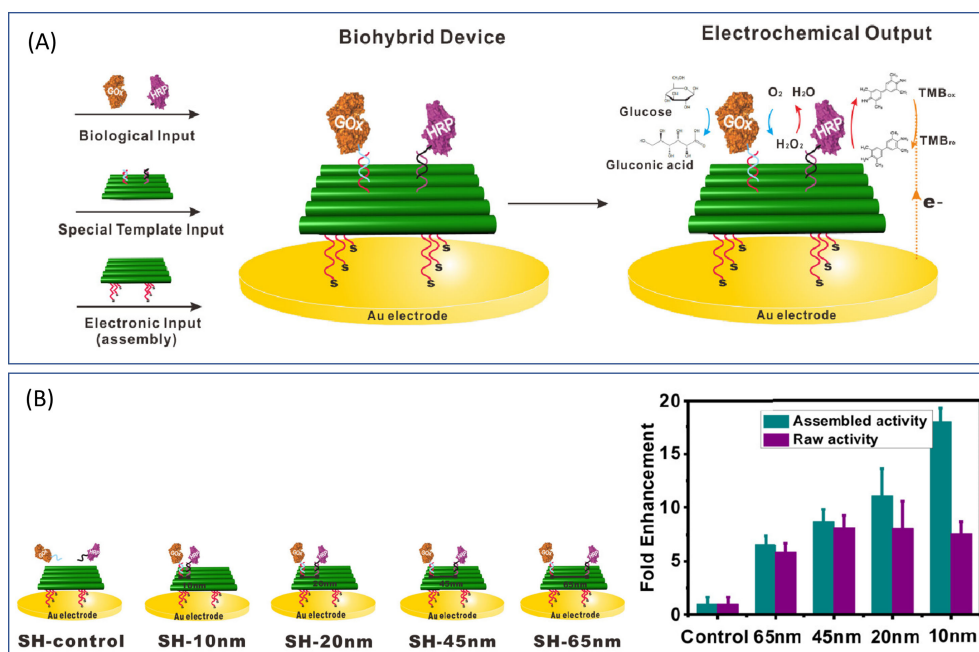


**Figure 15.** (A) scheme of the origami-based bioelectrode design. (B) Influence of inter-enzyme distance on the activity. Adapted with permission from.<sup>116</sup> Copyright 2019 American Chemical Society.

the DNA origami was the accumulation in the DNA strands of tetramethylbenzidine inducing an apparent enhancement of enzymatic activity. Enhanced activity was proposed to be linked to the coverage of DNA origami on the electrode that allows intermediate diffusion from one enzyme to the other on the same DNA rectangle but also to a neighbor DNA origami. This study suggests that the influence of distance between enzyme on the efficiency of the enzyme cascade would be predominant at the electrode surface compared to scaffolding in solution.

## 5. Conclusion and Perspectives

This short review aims at reporting the recent developments in electrode patterning for bioelectrocatalysis. The objective of such patterning is to control and understand the role of the spatial

distribution and scaffolding of biomolecules on electrocatalytic activity, with the main idea that electrocatalytic processes at the scale of the single molecule bring additional information compared to electrocatalysis at the ensemble scale. Furthermore, it is expected to offer environments mimicking physiological ones. Mixed layers forming films at electrodes with spatially controlled chemical functions appear to be the simplest way to achieve a patterning of the electrode surface. Those films are widely used in bioelectrocatalysis, and they are expected primarily to avoid enzyme steric hindrance. However, information about the spatial distribution at the molecular scale, and the consequences on electrocatalytic activity, is lacking in most cases. Patterning of the electrode material itself is another way toward the control of the spatial distribution of enzymes. Controlled spatial distribution of NPs should in principle be suitable for such patterning, although the simultaneous variation

of the NP size and density might be an obstacle to the overall understanding of the phenomena. Hierarchical porosity on the other hand might suffer from difficulties to image the whole volume. Lithography techniques are more and more diversified. They are developed mainly for applicative reasons so far, but they should bring great opportunities in the bioelectrocatalytic fundamental understanding. Finally, biomolecule platforms such as virus scaffolds or DNA origamis, offer a large variety of possibilities for surface patterning. Here, the current requirement is the extension of these tools toward electrochemistry, meaning the step of transferring these platforms on conductive surfaces must be completed. To reach the objective of spatial control of enzymes on electrodes, and ultimately the understanding of bioelectrocatalysis at the single molecule level, no doubt that it is mandatory to enhance the interdisciplinarity in this research, with combined expertise in chemistry, biology, optics, materials sciences and instrumentation.

### CRedit Authorship Contribution Statement

Umberto Contaldo: Writing – review & editing (Supporting)  
 Anne de Poulpiquet: Writing – review & editing (Supporting)  
 Ievgen Mazurenko: Writing – review & editing (Supporting)  
 Elisabeth Lojou: Conceptualization (Lead), Funding acquisition (Lead), Supervision (Lead), Writing – original draft (Lead), Writing – review & editing (Lead)

### Conflict of Interest

The authors declare no conflict of interest in the manuscript.

### Funding

Agence Nationale de la Recherche: MetCop-ANR-21-CE44-0024-01

### References

- C. Beaufils, H. M. Man, A. de Poulpiquet, I. Mazurenko, and E. Lojou, *Catalysts*, **11**, 497 (2021).
- K. Kano, *Biosci. Biotechnol. Biochem.*, **86**, 141 (2022).
- N. S. Herzallh, Y. Cohen, R. Cohen, O. Chmelnik, Y. Shoham, and O. Yechezkel, *Sustain. Energy Fuels*, **5**, 4580 (2021).
- Y. Suzuki, F. Makino, T. Miyata, H. Tanaka, K. Namba, K. Kano, K. Sowa, Y. Kitazumi, and O. Shirai, *ACS Catal.*, **13**, 13828 (2023).
- I. Mazurenko, V. P. Hitaishi, and E. Lojou, *Curr. Opin. Electrochem.*, **19**, 113 (2020).
- M. Tominaga, S. Tamai, S. Nakao, M. Miyamoto, and T. Satomura, *Electrochem. Commun.*, **136**, 107222 (2022).
- N. Lalaoui, K. Gentil, I. Ghandari, S. Cosnier, and F. Giroud, *Electrochim. Acta*, **408**, 139894 (2022).
- Y. Takahashi, M. Wanibuchi, Y. Kitazumi, O. Shirai, and K. Kano, *J. Electroanal. Chem.*, **843**, 47 (2019).
- V. P. Hitaishi, R. Clement, N. Bourassin, M. Baaden, A. de Poulpiquet, S. Sacquin-Mora, A. Ciaccavava, and E. Lojou, *Catalysts*, **8**, 192 (2018).
- W. Q. Chen, W. J. Wu, Y. Q. Yu, Y. Liu, and F. L. Jiang, *Langmuir*, **39**, 9595 (2023).
- D. Zigah, E. Lojou, and A. de Poulpiquet, *ChemElectroChem*, **6**, 5524 (2019).
- N. Kornienko, K. H. Ly, W. E. Robinson, N. Heidary, J. Z. Zhang, and E. Reisner, *Acc. Chem. Res.*, **52**, 1439 (2019).
- H. M. Man, I. Mazurenko, H. Le Guenno, L. Bouffier, E. Lojou, and A. de Poulpiquet, *Anal. Chem.*, **94**, 15604 (2022).
- V. Saska, U. Contaldo, I. Mazurenko, A. de Poulpiquet, and E. Lojou, *Bioelectrochemistry*, **153**, 108503 (2023).
- N. Zeballos, E. Diamanti, A. I. Benitez-Mateos, C. Schmidt-Dannert, and F. Lopez-Gallego, *Bioconjugate Chem.*, **32**, 1966 (2021).
- B. J. Johnson, W. R. Algar, A. P. Malanoski, M. G. Ancona, and I. L. Medintz, *Nano Today*, **9**, 102 (2014).
- T. Adachi, T. Miyata, F. Makino, H. Tanaka, K. Namba, K. Kano, K. Sowa, Y. Kitazumi, and O. Shirai, *ACS Catal.*, **13**, 7955 (2023).
- C. J. Delebecque, A. B. Lindner, P. A. Silver, and F. A. Aldaye, *Science*, **333**, 470 (2011).
- M. Rasmussen, S. Abdellaoui, and S. D. Minteer, *Biosens. Bioelectron.*, **76**, 91 (2016).
- Y. F. Zhang, S. Tsitkov, and H. Hess, *Nat. Commun.*, **7**, 13982 (2016).
- T. McArdle, T. P. McNamara, F. Fei, K. Singh, and C. F. Blanford, *ACS Appl. Mater. Interfaces*, **7**, 25270 (2015).
- C. Gutierrez-Sanchez, A. Ciaccavava, P. Y. Blanchard, K. Monsalve, M. T. Giudici-Ortoni, S. Lecomte, and E. Lojou, *ACS Catal.*, **6**, 5482 (2016).
- L. Zanetti-Polzi, I. Daidone, C. A. Bortolotti, and S. Corni, *J. Am. Chem. Soc.*, **136**, 12929 (2014).
- T. Wilhelm and G. Wittstock, *Angew. Chem., Int. Ed.*, **42**, 2248 (2003).
- Y. Takahashi, A. I. Shevchuk, P. Novak, Y. Murakami, H. Shiku, Y. E. Korchev, and T. Matsue, *J. Am. Chem. Soc.*, **132**, 10118 (2010).
- A. Anne, C. Demaille, and C. Goyer, *ACS Nano*, **3**, 819 (2009).
- B. Tassy, A. L. Dauphin, H. M. Man, H. Le Guenno, E. Lojou, L. Bouffier, and A. de Poulpiquet, *Anal. Chem.*, **92**, 7249 (2020).
- Y. Wu and N. Arroyo-Curras, *Curr. Opin. Electrochem.*, **27**, 100695 (2021).
- A. Ulman, *Chem. Rev.*, **96**, 1533 (1996).
- K. Tamada, M. Hara, H. Sasabe, and W. Knoll, *Langmuir*, **13**, 1558 (1997).
- J. C. Love, L. A. Estroff, J. K. Kriebel, R. G. Nuzzo, and G. M. Whitesides, *Chem. Rev.*, **105**, 1103 (2005).
- D. A. Sadik, H. Eksi-Kocak, G. Ertaş, I. H. Boyacı, and M. Mutlu, *Surf. Interface Anal.*, **50**, 866 (2018).
- R. M. Mayall, M. Renaud-Young, E. Gawron, S. Luong, S. Creager, and V. I. Birss, *ACS Sens.*, **4**, 143 (2019).
- F. Ricci, R. Y. Lai, A. J. Heeger, K. W. Plaxco, and J. J. Sumner, *Langmuir*, **23**, 6827 (2007).
- T. X. Ma, A. J. Grzedowski, T. Doneux, and D. Bizzotto, *J. Am. Chem. Soc.*, **144**, 23428 (2022).
- T. Utesch, J. Staffa, S. Katz, G. Y. Yao, J. Kozuch, and P. Hildebrandt, *J. Phys. Chem. B*, **126**, 7664 (2022).
- M. Kato, R. Sano, N. Yoshida, M. Iwafuji, Y. Nishiyama, S. Oka, K. Shinzawa-Itoh, Y. Nishida, Y. Shintani, and I. Yagi, *J. Phys. Chem. Lett.*, **13**, 9165 (2022).
- D. C. Kim, J. I. Sohn, D. J. Zhou, T. A. J. Duke, and D. J. Kang, *ACS Nano*, **4**, 1580 (2010).
- G. Di Rocco, G. Battistuzzi, A. Ranieri, C. A. Bortolotti, M. Borsari, and M. Sola, *Molecules*, **27**, 8079 (2022).
- P. Bollella, L. Gorton, R. Ludwig, and R. Antiochia, *Sensors*, **17**, 1912 (2017).
- N. Lokar, B. Pecar, M. Mozek, and D. Vrtacnik, *Biosensors (Basel)*, **13**, 364 (2023).
- C. Jiang, S. M. Silva, S. J. Fan, Y. F. Wu, M. T. Alam, G. Z. Liu, and J. J. Gooding, *J. Electroanal. Chem.*, **785**, 265 (2017).
- G. Z. Liu and J. J. Gooding, *Langmuir*, **22**, 7421 (2006).
- M. Cesbron, S. Dabos-Seignon, C. Gautier, and T. Breton, *Electrochim. Acta*, **345**, 136190 (2020).
- A. Pierro, A. Bonucci, D. Normanno, M. Ansaldi, E. Pilet, O. Ouari, B. Guigliarelli, E. Etienne, G. Gerbaud, A. Magalon, V. Belle, and E. Mileo, *Chem. Eur. J.*, **28**, e202202249 (2022).
- K. Abdiaziz, E. Salvadori, K. P. Sokol, E. Reisner, and M. M. Roessler, *Chem. Commun.*, **55**, 8840 (2019).
- F. A. Al-Lolage, M. Meneghello, S. Ma, R. Ludwig, and P. N. Bartlett, *ChemElectroChem*, **4**, 1528 (2017).
- F. A. Al-Lolage, P. N. Bartlett, S. Gounel, P. Staigre, and N. Mano, *ACS Catal.*, **9**, 2068 (2019).
- M. Holzinger, S. Cosnier, and P. H. M. Buzzetti, *Synth. Met.*, **292**, 117219 (2023).
- E. Takamura, T. Ohnishi, H. Sakamoto, T. Satomura, and S. Suye, *J. Phys. Energy*, **3**, 014006 (2021).
- D. Pankratov, R. Sundberg, J. Sotres, D. B. Suyatin, I. Maximov, S. Shleev, and L. Montelius, *Beilstein J. Nanotechnol.*, **6**, 1377 (2015).
- N. Karimian, D. Campagnol, M. Tormen, A. M. Stortini, P. Canton, and P. Ugo, *J. Electroanal. Chem.*, **932**, 117240 (2023).
- Y. Sugimoto, Y. Kitazumi, O. Shirai, and K. Kano, *Electrochemistry*, **85**, 82 (2017).
- Y. Sugimoto, R. Takeuchi, Y. Kitazumi, O. Shirai, and K. Kano, *J. Phys. Chem. C*, **120**, 26270 (2016).
- H. M. Wu, X. R. Zhang, C. J. Wei, C. C. Wang, M. Jiang, X. A. Hong, Z. K. Xu, D. J. Chen, and X. J. Huang, *Chem. Eng. J.*, **421**, 129721 (2021).
- I. Mazurenko, K. Monsalve, P. Infossi, M. T. Giudici-Ortoni, F. Topin, N. Mano, and E. Lojou, *Energy Environ. Sci.*, **10**, 1966 (2017).
- C. Mateo-Mateo, A. S. Michardière, S. Gounel, I. Ly, J. Rouhana, P. Poulin, and N. Mano, *ChemElectroChem*, **2**, 1908 (2015).
- H. X. Yang, X. F. Zhu, K. Hua, F. Z. Yuan, J. Zhang, and Y. C. Jiang, *Mol. Catal.*, **547**, 113290 (2023).
- M. Z. do Valle Gomes, G. Masdeu, P. Eiring, A. Kuhlemann, M. Sauer, B. Åkerman, and A. E. C. Palmqvist, *Catal. Sci. Technol.*, **11**, 6952 (2021).
- G. A. Ellis, S. A. Diaz, and I. L. Medintz, *Curr. Opin. Biotechnol.*, **71**, 77 (2021).
- W. Kang, J. H. Liu, J. P. Wang, Y. Y. Nie, Z. H. Guo, and J. Xia, *Bioconjugate Chem.*, **25**, 1387 (2014).
- K. Monsalve, M. Roger, C. Gutierrez-Sanchez, M. Ilbert, S. Nitsche, D. Byrne-Kodjabachian, V. Marchi, and E. Lojou, *Bioelectrochemistry*, **106**, 47 (2015).
- Y. Mie, H. Okabe, C. Mikami, T. Motomura, and N. Matsuda, *Electrochem. Commun.*, **146**, 107415 (2023).
- M. Suzuki, K. Murata, N. Nakamura, and H. Ohno, *Electrochemistry*, **80**, 337

- (2012).
65. H. Lee, Y. S. Lee, S. K. Lee, S. Baek, I. G. Choi, J. H. Jang, and I. S. Chang, *Biosens. Bioelectron.*, **126**, 170 (2019).
  66. V. P. Hitaisi, I. Mazurenko, M. A. Vengasseril, A. de Poulpiquet, G. Coustillier, P. Delaporte, and E. Lojou, *Front Chem.*, **8**, 431 (2020).
  67. W. Lipińska, K. Siuzdak, J. Karczewski, A. Dołęga, and K. Grochowska, *Sens. Actuators, B*, **330**, 129409 (2021).
  68. W. Lipińska, V. Saska, K. Siuzdak, J. Karczewski, K. Załęski, E. Coy, A. de Poulpiquet, I. Mazurenko, and E. Lojou, *Electrochim. Acta*, **474**, 143535 (2024).
  69. A. C. Jahns and B. H. A. Rehm, *Microb. Biotechnol.*, **5**, 188 (2012).
  70. J. X. Song, B. Liang, D. F. Han, X. J. Tang, Q. L. Lang, R. R. Feng, L. H. Han, and A. H. Liu, *Enzyme Microb. Technol.*, **70**, 72 (2015).
  71. Y. Y. Chen, B. Stemple, M. Kumar, and N. Wei, *Environ. Sci. Technol.*, **50**, 8799 (2016).
  72. M.-L. Pham and M. Polakovič, *Int. J. Biol. Macromol.*, **165**, 835 (2020).
  73. L. Chen, A. Mulchandani, and X. Ge, *Biotechnol. Prog.*, **33**, 383 (2017).
  74. L. Han, B. Liang, and J. X. Song, *J. Ind. Microbiol. Biotechnol.*, **45**, 111 (2018).
  75. A. S. Wiczorek and V. J. J. Martin, *Microb. Cell Fact.*, **9**, 69 (2010).
  76. F. Liu, S. Banta, and W. Chen, *Chem. Commun.*, **49**, 3766 (2013).
  77. S. Shibasaki and M. Ueda, *Biocontrol Sci.*, **19**, 157 (2014).
  78. B. Liang, L. Li, X. L. Tang, Q. L. Lang, H. W. Wang, F. Li, J. G. Shi, W. Shen, I. Palchetti, M. Mascini, and A. H. Liu, *Biosens. Bioelectr.*, **45**, 19 (2013).
  79. B. Liang, S. Zhang, Q. L. Lang, J. X. Song, L. H. Han, and A. H. Liu, *Anal. Chim. Acta*, **884**, 83 (2015).
  80. Z. Zhang, J. Liu, J. Fan, Z. Y. Wang, and L. Li, *Anal. Chim. Acta*, **1009**, 65 (2018).
  81. L. Xia, B. Liang, L. Li, X. J. Tang, I. Palchetti, M. Mascini, and A. H. Liu, *Biosens. Bioelectron.*, **44**, 160 (2013).
  82. S. Fishilevich, L. Amir, Y. Fridman, A. Aharoni, and L. Alfonta, *J. Am. Chem. Soc.*, **131**, 12052 (2009).
  83. I. Gal, O. Schlesinger, L. Amir, and L. Alfonta, *Bioelectrochemistry*, **112**, 53 (2016).
  84. X. X. Xiao, H. Q. Xia, R. R. Wu, L. Bai, L. Yan, E. Magner, S. Cosnier, E. Lojou, Z. G. Zhu, and A. H. Liu, *Chem. Rev.*, **119**, 9509 (2019).
  85. A. Szczupak, D. Aizik, S. Morais, Y. Vazana, Y. Barak, E. A. Bayer, and L. Alfonta, *Nanomaterials*, **7**, 153 (2017).
  86. S. Q. Fan, B. Liang, X. X. Xiao, L. Bai, X. J. Tang, E. Lojou, S. Cosnier, and A. H. Liu, *J. Am. Chem. Soc.*, **142**, 3222 (2020).
  87. J. Pille, D. Cardinale, N. Carette, C. Di Primo, J. Besong-Ndika, J. Walter, H. Lecoq, M. B. van Eldijk, F. C. M. Smits, S. Schoffelen, J. C. M. van Hest, K. Mäkinen, and T. Michon, *Biomacromolecules*, **14**, 4351 (2013).
  88. D. S. Petrescu, O. K. Zahr, I. Abu-Baker, and A. S. Blum, *Biomacromolecules*, **23**, 3407 (2022).
  89. M. Bäcker, C. Koch, S. Eiben, F. Geiger, F. Eber, H. Gliemann, A. Poghossian, C. Wege, and M. J. Schöning, *Sens. Actuators, B*, **238**, 716 (2017).
  90. N. Bhokisham, Y. Liu, A. D. Brown, G. F. Payne, J. N. Culver, and W. E. Bentley, *Biofabrication*, **12**, 045017 (2020).
  91. R. A. Blaik, E. Lan, Y. Huang, and B. Dunn, *ACS Nano*, **10**, 324 (2016).
  92. S. J. White, S. Johnson, M. Szymonik, R. A. Wardingley, D. Pye, A. G. Davies, C. Wälti, and P. G. Stockley, *Nanotechnology*, **23**, 495304 (2012).
  93. A. Chovin, C. Demaille, and T. O. Paiva, *Curr. Opin. Electrochem.*, **40**, 101346 (2023).
  94. L. Nault, C. Taofifenua, A. Anne, A. Chovin, C. Demaille, J. Besong-Ndika, D. Cardinale, N. Carette, T. Michon, and J. Walter, *ACS Nano*, **9**, 4911 (2015).
  95. A. N. Patel, A. Anne, A. Chovin, C. Demaille, E. Grelet, T. Michon, and C. Taofifenua, *Small*, **13**, 1603163 (2017).
  96. K. Torbensen, A. N. Patel, A. Anne, A. Chovin, C. Demaille, L. Bataille, T. Michon, and E. Grelete, *ACS Catal.*, **9**, 5783 (2019).
  97. T. O. Paiva, K. Torbensen, A. N. Patel, A. Anne, A. Chovin, C. Demaille, L. Bataille, and T. Michon, *ACS Catal.*, **10**, 7843 (2020).
  98. T. O. Paiva, A. Schneider, L. Bataille, A. Chovin, A. Anne, T. Michon, C. Wege, and C. Demaille, *Nanoscale*, **14**, 875 (2022).
  99. R. Kassem, A. Cousin, D. Clesse, V. Poignavent, A. Trolet, C. Ritzenthaler, T. Michon, A. Chovin, and C. Demaille, *Bioelectrochemistry*, **155**, 108570 (2024).
  100. D. D. Zeng, L. L. San, F. Y. Qian, Z. L. Ge, X. H. Xu, B. Wang, Q. Li, G. F. He, and X. Q. Mi, *ACS Appl. Mater. Interfaces*, **11**, 21859 (2019).
  101. P. W. K. Rothemund, *Nature*, **440**, 297 (2006).
  102. N. C. Seeman and H. F. Sleiman, *Nat. Rev. Mater.*, **3**, 17068 (2018).
  103. W. J. Wang, S. Yu, S. Huang, S. Bi, H. Y. Han, J. R. Zhang, Y. Lu, and J. J. Zhu, *Chem. Soc. Rev.*, **48**, 4892 (2019).
  104. J. X. Wu, Y. C. Qu, Q. Yu, and H. Chen, *Mater. Chem. Front.*, **2**, 2175 (2018).
  105. A. Rajendran, E. Nakata, S. Nakano, and T. Morii, *ChemBioChem*, **18**, 696 (2017).
  106. M. Vázquez-González, C. Wang, and I. Willner, *Nat. Catal.*, **3**, 256 (2020).
  107. V. Linko, M. Eerikainen, and M. A. Kostianen, *Chem. Commun.*, **51**, 5351 (2015).
  108. Y. H. Chen, G. L. Ke, Y. L. Ma, Z. Zhu, M. H. Liu, Y. Liu, H. Yan, and C. J. Yang, *J. Am. Chem. Soc.*, **140**, 8990 (2018).
  109. J. L. Fu, M. H. Liu, Y. Liu, N. W. Woodbury, and H. Yan, *J. Am. Chem. Soc.*, **134**, 5516 (2012).
  110. J. S. Kahn, Y. Xiong, J. Huang, and O. Gang, *JACS Au*, **2**, 357 (2022).
  111. L. Xia, K. V. Nguyen, Y. Holade, H. Han, K. Dooley, P. Atanassov, S. Banta, and S. D. Minter, *ACS Energy Lett.*, **2**, 1435 (2017).
  112. Z. L. Ge, Z. M. Su, C. R. Simmons, J. Li, S. X. Jiang, W. Li, Y. Yang, Y. Liu, W. Chiu, C. H. Fan, and H. Yan, *ACS Appl. Mater. Interfaces*, **11**, 13874 (2019).
  113. E. Pensa, Y. Bogawat, F. C. Simmel, and I. Santiago, *ChemElectroChem*, **9**, e202101696 (2022).
  114. S. Han, W. Y. Liu, S. Yang, and R. S. Wang, *ACS Omega*, **4**, 11025 (2019).
  115. N. Arroyo-Currás, M. Sadeia, A. K. Ng, Y. Fyodorova, N. Williams, T. Afif, C.-M. Huang, N. Ogden, R. C. A. Eguiluz, H.-J. Su, C. E. Castro, K. W. Plaxco, and P. S. Lukeman, *Nanoscale*, **12**, 13907 (2020).
  116. Z. L. Ge, J. L. Fu, M. H. Liu, S. X. Jiang, A. Andreoni, X. L. Zuo, Y. Liu, H. Yan, and C. H. Fan, *ACS Appl. Mater. Interfaces*, **11**, 13881 (2019).